the plant journal

SEB SOCIETY FOR EXPERIMENTAL BIOLOGY

The Plant Journal (2023) doi: 10.1111/tpj.16140

Transcriptome analysis of the phosphate starvation response sheds light on strigolactone biosynthesis in rice

Imran Haider[1,2], Zhang Yunmeng[3], Fred White[1], Changsheng Li[1], Roberto Incitti[4], Intikhab Alam[4], Takashi Gojobori[4], Carolien Ruyter-Spira[3], Salim Al-Babili[2,5,*] and Harro J. Bouwmeester[1,*]

[1]*Plant Hormone Biology Group, Swammerdam Institute for Life Sciences, University of Amsterdam, Science Park 904, 1098 XH, Amsterdam, The Netherlands,*

[2]*Division of Biological and Environmental Science and Engineering, Center for Desert Agriculture, The BioActives Lab, King Abdullah University of Science and Technology, Thuwal 23955-6900, Saudi Arabia,*

[3]*Laboratory of Plant Physiology, Wageningen University and Research, Wageningen, PO Box 658, 6700 AR, The Netherlands,*

[4]*Computational Bioscience Research Center, King Abdullah University of Science and Technology, Thuwal 23955-6900, Saudi Arabia, and*

[5]*Division of Biological and Environmental Science and Engineering, The Plant Science Program, King Abdullah University of Science and Technology, Thuwal 23955-6900, Saudi Arabia*

Received 12 September 2022; accepted 6 February 2023.
*For correspondence (e-mail salim.babili@kaust.edu.sa; h.j.bouwmeester@uva.nl).

SUMMARY

Phosphorus (P) is a major element required for plant growth and development. To cope with P shortage, plants activate local and long-distance signaling pathways, such as an increase in the production and exudation of strigolactones (SLs). The role of the latter in mitigating P deficiency is, however, still largely unknown. To shed light on this, we studied the transcriptional response to P starvation and replenishment in wild-type rice and a SL mutant, *dwarf10* (*d10*), and upon exogenous application of the synthetic SL GR24. P starvation resulted in major transcriptional alterations, such as the upregulation of *P TRANSPORTER*, *SYG1/PHO81/XPR1* (*SPX*) and *VACUOLAR PHOSPHATE EFFLUX TRANSPORTER*. Gene Ontology (GO) analysis of the genes induced by P starvation showed enrichment in phospholipid catabolic process and phosphatase activity. In *d10*, P deficiency induced upregulation of genes enriched for sesquiterpenoid production, secondary shoot formation and metabolic processes, including lactone biosynthesis. Furthermore, several genes induced by GR24 treatment shared the same GO terms with P starvation-induced genes, such as oxidation reduction, heme binding and oxidoreductase activity, hinting at the role that SLs play in the transcriptional reprogramming upon P starvation. Gene co-expression network analysis uncovered a *METHYL TRANSFERASE* that displayed co-regulation with known rice SL biosynthetic genes. Functional characterization showed that this gene encodes an enzyme catalyzing the conversion of carlactonoic acid to methyl carlactonoate. Our work provides a valuable resource to further studies on the response of crops to P deficiency and reveals a tool for the discovery of SL biosynthetic genes.

Keywords: methyl transferase, phosphate starvation, RNA-sequencing, Rice (*Oryza sativa*), Strigolactone biosynthesis.

INTRODUCTION

Phosphorus is assimilated by plants for growth and development, predominantly in the form of inorganic phosphate (P). P availability to plants is often limited because of rapid immobilization and slow diffusion (Rouached et al., 2010; Yang & Finnegan, 2010). P fertilizer application overcomes this and improves crop yield but causes environmental issues and is not sustainabile. Heavy fertilizer use may cause eutrophication and the P rock resource is limited (Jama-Rodzeńska et al., 2021). Therefore, it is important to study and improve P uptake and P use efficiency of crops.

Plants have evolved morphological, physiological, biochemical and molecular adaptations to respond to P starvation (López-Arredondo et al., 2014; Yang & Finnegan, 2010). These mechanisms include sensing external and internal P concentrations, which are translated into local

and long-distance signaling pathways that result in downstream local and systemic responses. Transporters play an important role in P acquisition and (re-)allocation (Gu et al., 2016). Collectively, P starvation responses (PSRs) help plants to enhance the acquisition of external P as well as to conserve and mobilize internal P (Chien et al., 2018; Zhang, Liao, & Lucas, 2014).

When growing under P-deficiency, plant roots tend to be concentrated in the topsoil. This local response is achieved by inhibition of primary root elongation and stimulation of lateral root initiation and outgrowth, which is under complex genetic and hormonal control (Crombez et al., 2019; Ham et al., 2018). In addition to adapted root architecture, increased root exudation of P solubilizing compounds and induction of P transporters can help plants to improve their P acquisition efficiency (Heuer et al., 2017; Liang et al., 2014).

Plants rely on P transporters to sense, acquire, translocate and remobilize P in the various organs (Wang, Kuo, & Chiou, 2021). P homeostasis is commonly regulated through direct or indirect regulation of the abundance of P transporters at the cellular, tissue and whole-plant level (Abel, 2017; Crombez et al., 2019; Gu et al., 2016; Puga et al., 2017). There are generally four groups of P transporters: the P TRANSPORTER (PHT) family, the SYG1/PHO81/XPR1 (SPX)-containing protein family, the PLASTIDIC PHOSPHORYLATED COMPOUNDS/P ANTIPORTERS and SULTR-like P transporters. P transport is highly regulated through transcriptional and post-transcriptional components, especially by P availability (Kopriva & Chu, 2018; Wang, Kuo, & Chiou, 2021). The SPXs have an important role in regulating P signaling- and homeostasis by binding to inositol pyrophosphates (Jung et al., 2018; Wild et al., 2016).

Strigolactones (SLs) play a crucial role in the plant response to P deficiency, in coordination with other hormones (Al-Babili & Bouwmeester, 2015; Crombez et al., 2019). SLs can act as rhizospheric signals to regulate the interaction of host plants with beneficial microbes and are abused by root parasitic plants (Bouwmeester et al., 2021; Lanfranco et al., 2018; López-Ráez et al., 2017). Beside their exogenous role in the rhizosphere, SLs act as a hormone to regulate several developmental processes that adapt plant architecture to nutrient availability (Aliche et al., 2020). Under various abiotic stresses, SLs accumulate, which in turn promotes plant tolerance and resilience (Dell'Oste et al., 2021; Haider et al., 2018; Mostofa et al., 2018; Pandey et al., 2016).

Many recent reviews have extensively discussed SL biosynthesis, perception and signal transduction (Bouwmeester et al., 2021; Bürger & Chory, 2020; Makhzoum et al., 2017; Waters et al., 2017; Yoneyama & Brewer, 2021). Therefore, here, we only briefly introduce this, focusing mostly on the regulation of the SL pathway under P deficiency and the mechanisms underlying SL-mediated plant adaption to P starvation. SLs derive from the carotenoid pathway (Matusova et al., 2005). Located upstream of the carotenoids is the 2C-METHYL-D-ERYTHRITOL-4-PHOSPHATE (MEP) pathway (Nisar et al., 2015). A family of CAROTENOID CLEAVAGE DIOXYGENASEs (CCDs) and 9-*cis*-EPOXYCAROTENOID DIOXYGENASEs (NCEDs) with different substrate preferences catalyzes carotenoid cleavage resulting in the biosynthesis of two closely related and interacting phytohormones, SLs and ABA, respectively. NCEDs catalyze oxidative cleavage of both 9-*cis*-violaxanthin and 9′-*cis*-neoxanthin into xanthoxin, the precursor of ABA, whereas CCD7 and 8 catalyze the sequential cleavage and conversion of 9-*cis*-β-carotene en route to SLs (Alder et al., 2012; Moreno et al., 2021). SL biosynthesis starts with the reversible isomerization of all-*trans*-β-carotene by *trans*/9-*cis*-β-carotene isomerase DWARF27 (D27) (Abuauf et al., 2018; Bruno & Al-Babili, 2016; Lin et al., 2009). 9-*cis*-β-Carotene is then sequentially cleaved and converted by CCD7 and CCD8 into carlactone (CL), a key intermediate in SL biosynthesis (Alder et al., 2012; Bruno et al., 2014, 2017). Further modifications of CL, such as hydroxylation and oxidation, catalyzed by cytochrome P450s (CYP450s) and other types of enzymes, including MORE AXILLARY GROWTH1 (MAX1) and LATERAL BRANCHING OXIDOREDUCTASE (LBO) (Brewer et al., 2016; Jia et al., 2018), result in the formation of different types of SLs.

Rice has been used several times as a model to study the transcriptional response of plants to P deficiency to find strategies for improving P acquisition and utilization (Oono et al., 2011, 2013). A more comprehensive RNA-sequencing (RNA-seq) study, including early and late stages of P starvation and replenishment in rice root and shoot, was carried out by (Secco et al., 2013). Two P starvation upregulated candidate genes from a comprehensive RNA-seq study by Gho et al. (2018), *SULFOQUINOVOSYL DIACYLGLYCEROL SYNTHASE2* (*SQD2*) and *PHOSPHATE TRANSPORTER6* (*PT6*), were overexpressed in rice and this enhanced P use efficiency (Gho et al., 2018). The latter studies focussed on the seedling/vegetative stage, whereas Jeong et al. (2017, 2018) studied the rice flag leaf transcriptome for P remobilization associated gene expression changes upon P starvation during the grain filling stage, and concluded that *PURPLE ACID PHOSPHATASEs* (*PAPs*) and *SPX* family genes contribute to the remobilization of P from senescing flag leaves to developing grains.

Transcriptome studies on the response to SLs have been performed in many plant species, including rice, using the synthetic SL analog GR24 (Makhzoum et al., 2017; Wang, Duran, et al., 2021; Zhou et al., 2020). In the present study, we compared the P deficiency and GR24 response in one study. Accordingly, we performed in-depth temporal transcriptome analysis using RNA-seq,

covering a time span of P deficiency in roots of wild-type rice and the SL deficient mutant *d10*- defective in *CCD8*. Moreover, we applied P replenishment and GR24 as controls for the P deficiency and SL mutant treatments. Analysis of the RNA-seq data upon treatments at different time points provides a comprehensive overview of the dynamic responses of rice to P stress and how SLs are involved in this response at the transcriptome level. Through gene co-expression network analysis, we identified two putative *METHYL TRANSFERASE* genes. Functional studies of the corresponding enzymes in *Nicotiana benthamiana* revealed that they catalyze the conversion of carlactonoic acid (CLA) into methyl carlactonoate (MeCLA), an important step in non-canonical SL biosynthesis.

RESULTS AND DISCUSSION

The transcriptome of rice roots responds strongly to P starvation and replenishment

The average total reads for all samples was 10 152 732 with an average length of 251 bp. Within these, around 4.5% mapped to multiple loci and 2.8% mapped to too many loci (more than 10) on the reference rice genome (RAP-DB). Uniquely mapped reads accounted for an average of 81% of the total reads in each sample, with 0% chimeras. Altogether, these values indicate adequate pre-processing parameters (Table S1).

Principal component analysis (PCA) showed that the transcriptome response to the treatments was highly reproducible, with the biological replicates clustering closely together (Figure 1a). The effect of P starvation gradually increased at 1, 3, 7 and 8 days after treatment (DAT) with the starvation treatments clustering increasingly further away from the control. Just 1 day of P resupply at day 8, however, changed the P deficiency gene expression pattern back to the control treatment (Figure 1a), showing that the treatment effects were indeed strongly P-dependent.

To confirm the validity of RNA-seq, we randomly selected seven differentially expressed genes (DEGs) for quantitative real-time polymerase chain reaction (qRT-PCR) analysis, upon P starvation and P resupply at day 8. The qRT-PCR results were in good agreement with the $\log_2$ fold

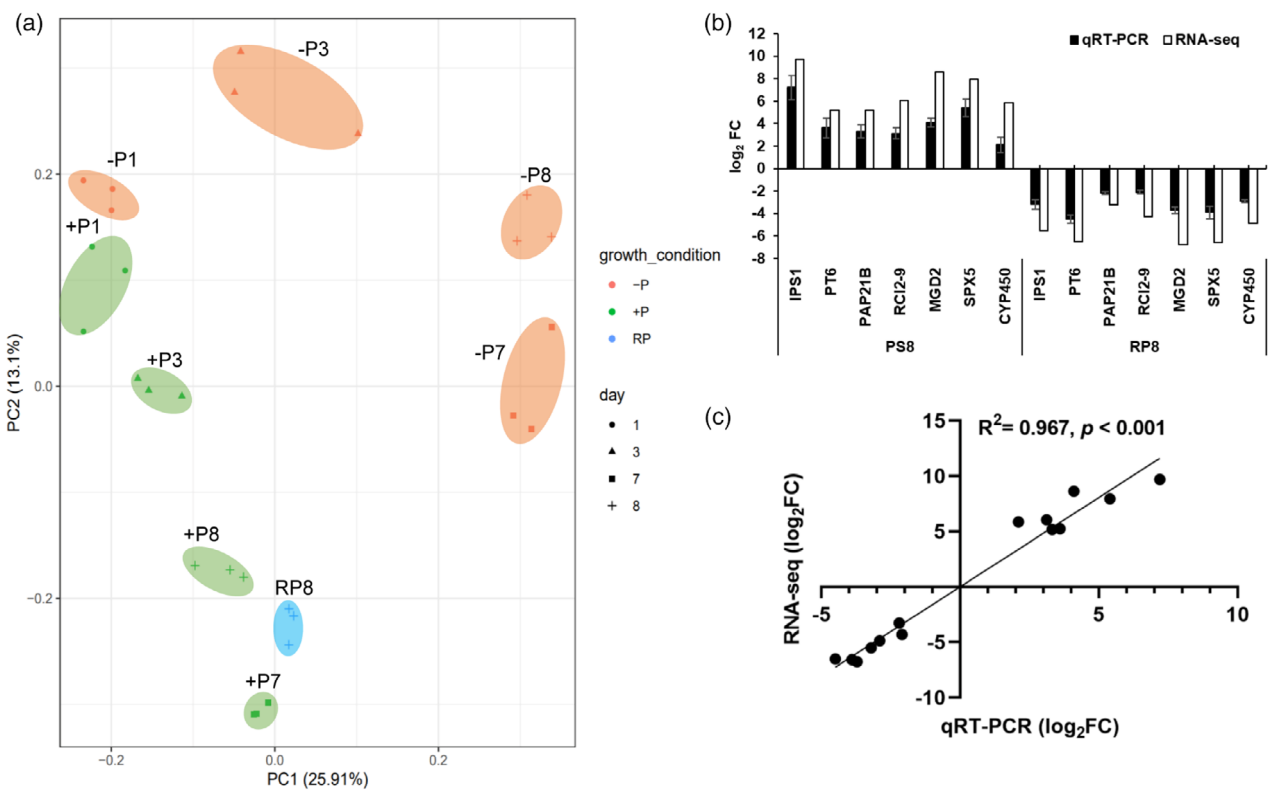

Figure 1. Validation of RNA-seq results in wild-type rice roots under P starvation and P replenishment.
(a) Principal component analysis of rice transcript profiles using DESeq2 transformed counts. Day 1, 3, 7 and 8 represent 1, 3, 7 and 8 days, respectively of P sufficient (+P) and P starvation (–P). RP represents 1 day of +P resupply after 7 days of –P. (b, c) Comparison of RNA-seq and qRT-PCR data of seven randomly selected genes at 8 days of –P (PS8) and RP8. Bars represent the mean ± SD (n = 3 biological replicates). *IPS1, PHOSPHATE STARVATION1* (*Os03g0146800*); *PT6, PHOSPHATE TRANSPORTER6,* (*Os08g0564000*); *PAP21B, PURPLE ACID PHOSPHATASE21B* (*Os11g0151700*); *OsRCI2-9, RARE COLD INDUCIBLE2* (*Os06g0651900*); *MGD2, MONOGALACTOSYLDIACYLGLYCEROL SYNTHASE2* (*Os08g0299400*); *SPX5, SYG1/PHO81/XPR1-5* (*Os03g0406100*). *CYP450, CYTOCHROME P450 PUTATIVE* (*Os10g0378100*). (c) A Pearson correlation coefficient of 0.967 is observed between the RNA-seq and qRT-PCR data of seven genes.

The Plant Journal published by Society for Experimental Biology and John Wiley & Sons Ltd.,
The Plant Journal, (2023), doi: 10.1111/tpj.16140

change (FC) values of the RNA-seq data (Figure 1b). Pearson correlation analysis revealed that the correlation was high and significant (Pearson correlation coefficient, R^2 = 0.96, $P < 0.001$) (Figure 1c), showing that the RNA-seq data are suitable for further analysis.

To analyze the effects of our treatments on gene expression, we identified DEGs between P starvation (and P replenishment) and the respective controls using DESEQ2 (Love et al., 2014) and threshold criteria of $\log_2$FC ≥1.2 and $P < 0.05$ (Figure 2; Data S1). P starvation resulted in 77 significantly differentially expressed genes at 1 DAT (29 genes up; 48 down), which is in the range of an earlier report (Secco et al., 2013). Likewise, a recent study in tomato showed that 2 days of P starvation resulted in 58 DEGs (Wang, Duran, et al., 2021). A sharp increase in the number of DEGs was observed at later stages of P starvation with 282 genes up and 385 down at 3 DAT (Figure 2b,f,g); 533 genes up and 507 down at 7 DAT (Figure 2c,f,g) and 906 genes up and 545 down at 8 DAT (Figure 2d,f,g). At 3 DAT, the expression of a number of known PSR genes

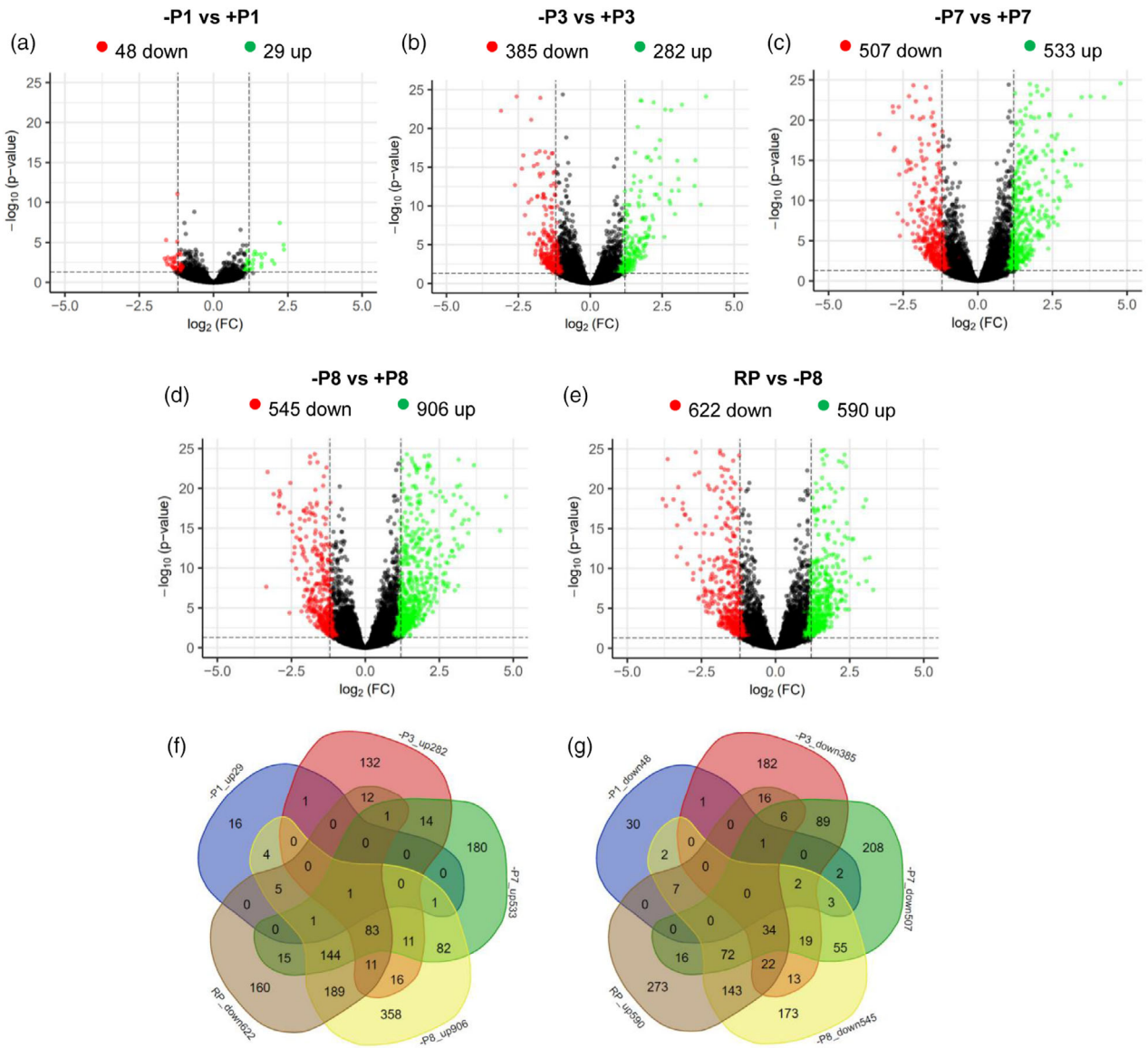

Figure 2. Number of significantly differentially expressed genes (DEGs) in wild-type rice roots at different time points of P starvation (–P) and + P resupply. (a–e) Volcano plots at (a) 1 day of –P, –P1 versus +P1, (b) 3 days of –P, –P3 versus +P3, (c) 7 days of –P, –P7 versus +P7, (d) 8 days of –P, –P8 versus +P8 and (e) 1 day of +P resupply after 7 days of –P (RP8 versus –P8). $P < 0.05$; $\log_2$FC ≥ 1.2. Red dots indicate significant number of downregulated genes, green dots indicate significant number of upregulated genes and black dots indicate genes that did not pass the threshold filters. (f, g) Venn diagrams of (f) upregulated and (g) downregulated genes. –P1, –P3, –P7 and –P8 represent DEGs of comparisons –P1 versus +P1, –P3 versus +P3, –P7 versus +P7 and –P8 versus +P8, respectively. RP represents RP8 versus –P8.

was already induced, and this induction increased at 7 and 8 DAT. The expression levels of *P TRANSPORTER* (*PT*) *1*, *2*, *6* and *8*, *SYG1/PHO81/XPR1* (*SPX*) *2* and *5*, *SPX-MFS2* (*MAJOR FACILITATOR SUPERFAMILY2*), *VACUOLAR PHOSPHATE EFFLUX TRANSPORTER* (*VPE*) *1* and *2*, and *NON-SPECIFIC PHOSPHOLIPASE C3* (*NPC3*) were highly upregulated by P starvation (Figure S1; Data S2). Upon P replenishment, all of these upregulated genes were repressed, confirming their dependence on P availability (Figure S1). Indeed, there is a strong transcriptional reprogramming upon P replenishment with 1212 genes changing expression compared to the continued P starvation treatment (622 genes down, 590 up; Figure 2e–g).

To gain a broader view of the differential gene expression under P deficiency, we carried out Gene Ontology (GO) (http://geneontology.org) enrichment analysis. GO terms were categorized into molecular function (MF), biological process (BP) and cellular component (CC) (Data S3). At day 1, there were no significantly enriched GO terms yet as a result of the limited number of DEGs. At 3, 7 and 8 DAT, in MF, the dominant group in enriched terms for the induced DEGs included 'phosphoric ester hydrolase activity', 'hydrolase activity acting on ester bonds' and 'phosphatase activity' (Figure S2; Data S3). The enriched terms for the upregulated DEGs in BP were 'lipid metabolic' and 'isoprenoid biosynthetic process' (Figure S2; Data S3). Enrichment in 'phospholipid catabolic process' and 'catalytic activity' appeared in the later stage of P starvation, at day 7 and 8 (Figure 3a; Data S1). The downregulated DEGs at day 3 of P starvation were enriched mainly in 'photosynthesis' and 'oxidoreductase activity' terms, consistent with the study by Secco et al. (2013). Interestingly, analysis of the 181 downregulated DEGs common for day 7 and 8 showed enrichment for 'nitric oxide'- and 'nicotianamine metabolic process' (Figure S2; Data S3). This result is in agreement with earlier work on rice and tomato showing that nitrogen (N) metabolic process is reduced under P starvation (Oono et al., 2013; Secco et al., 2013; Wang, Duran, et al., 2021). Genes *Os02g0770800* and *Os08g0468100*, both encoding a nitrate reductase, were downregulated by P starvation (Figure S3b; Data S3). Both genes were previously shown to be strongly repressed by N deficiency as well (Hsieh et al., 2018). An interaction between P and N to regulate PSR has been reported in several species such as *Arabidopsis*, rice and soyabean (Cai et al., 2013; Medici et al., 2019; Zhu et al., 2016).

Strigolactone biosynthesis and signaling respond to P status

Considering that SL production increases under P deficiency (Jamil et al., 2011; López-Ráez et al., 2008), it is not

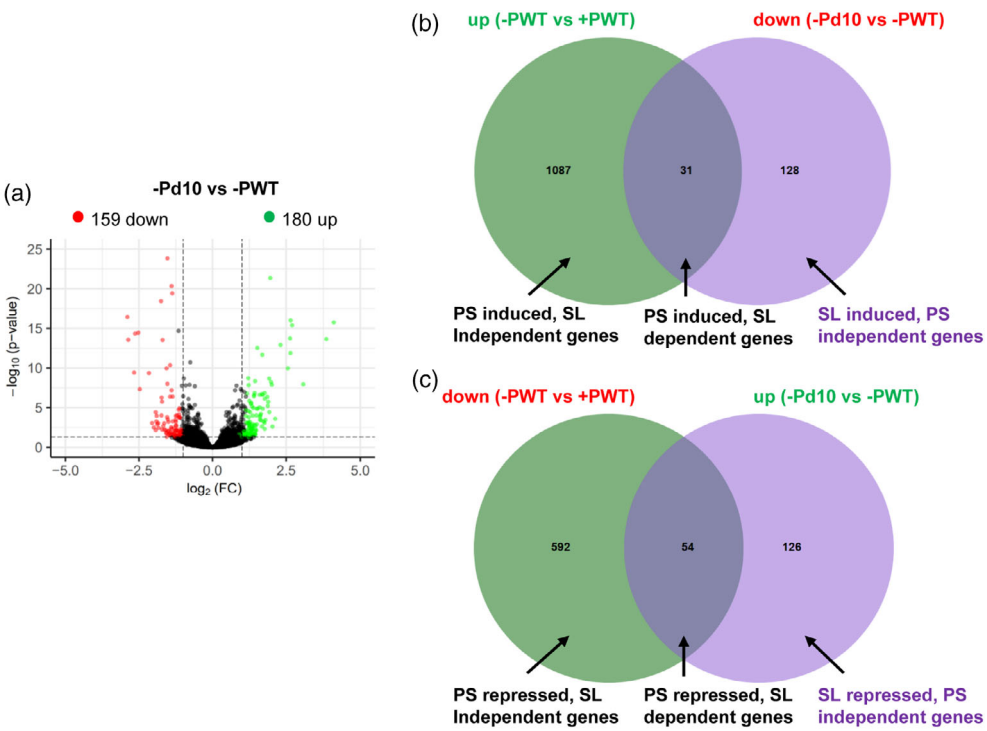

Figure 3. Volcano plots and Venn diagrams illustrating DEGs in the *d10* mutant compared to wild-type.
(a) Volcano plots in *d10* mutant compared to wild-type at day 8 (8 days of P starvation, –P*d10* versus –PWT). Red dots indicate significant number of downregulated genes, green dots indicate significant number of upregulated genes and black dots indicate genes that did not pass the threshold filters. (b, c) Venn diagrams showing the of number of up-and downregulated DEGs, respectively in wild-type (8 days of P starvation, –PWT versus +PWT) and down-and upregulated DEGs, respectively in the *d10* mutant compared to wild-type (8 days of P starvation, –Pd10 versus –PWT). $P < 0.05$; $\log_2 FC \geq 1.0$.

The Plant Journal published by Society for Experimental Biology and John Wiley & Sons Ltd.,
The Plant Journal, (2023), doi: 10.1111/tpj.16140

surprising that the expression of SL biosynthetic genes is induced by P starvation (Umehara et al., 2010). To study this effect in more detail, we compared changes in the expression of SL biosynthetic and signaling genes across the four time points of P starvation and P replenishment (Figure S1; Data S2). The SL biosynthetic genes *DWARF27* (*D27*), *CCD7* and *CCD8* and rice *MAX1* homolog *Os900/CYP711A2* were upregulated in all time points of P starvation, except at 1 DAT. Transcript levels of zaxinone biosynthetic gene *ZAXINONE SYNTHASE* (*ZAS*), and GRAS-type transcription factors *NODULATION SIGNALING PATHWAY1* (*NSP1*) and *NSP2* that control SL biosynthesis (Liu et al., 2011; Wang, Haider, et al., 2019), were also induced. SL biosynthetic genes expression was repressed again upon 1 day of P resupply at day 8 (Figure S1).

Expression of the SL receptor *DWARF14* (*D14*) displayed an opposite trend: it was significantly repressed by P starvation and then induced by 1 day of P resupply (Figure S1; Data S2). This expression pattern of *D14* was also recently reported in tomato (Wang, Duran, et al., 2021). Expression of the downstream signaling components F-box *DWARF3* (*D3*) and the repressor of SL signaling *DWARF53* (*D53*) did not display a consistent pattern (Wang, Duran, et al., 2021).

Strigolactones affect the transcriptional response to P starvation

To better understand the role of SLs in the P starvation response, we next compared the transcriptional changes in response to P starvation in the *d10* mutant and the effect of GR24 application, all on 8 DAT. PCA shows that the first two principal components explain over 48% of the variation in gene expression between the samples at day 8 (Figure S3). The replicates of the treatments cluster together closely, and there is a clear P starvation effect, also in *d10*. The difference in gene expression between wild-type and *d10* under P deficiency is small (Figure S3). To have sufficient DEGs for GO analyses, we therefore dropped the cut-off $\log_2$FC value to 1.0 in contrast to the rest of our analyses where we used $\log_2$FC 1.2. Volcano plots and a Venn diagram show that 180 and 159 DEGs were up- and downregulated, respectively, by 8 days of P starvation in *d10* compared to wild-type (Figure 3a; Data S4).

To further narrow down which P starvation-induced DEGs are dependent on SLs, we divided the DEGs into two Venn diagrams (Figure 3b,c). Figure 3b shows the 8 days of P starvation upregulated DEGs in wild-type and the downregulated DEGs in *d10* revealing 128 DEGs that are SL induced, independent of P starvation (Figure 3b). These DEGs are significantly enriched in 'ADP binding' and 'isoprenoid biosynthetic- and metabolic process' (Figure S5a; Data S5). In the overlapping region, the Venn diagram shows 31 DEGs that are induced by P starvation in a SL-dependent manner (Figure 3b). Interestingly, there are several transcription factors (TFs) among these 31 DEGs, such as *BASIC LEUCINE-ZIPPER*, *Zinc-finger*, *HEAT STRESS-TF* and *MADS-box*, which are induced by P starvation in wild-type but are repressed in *d10* compared to wild-type, suggesting that SL is needed for their induction (Data S5).

The second Venn diagram presents the 8 days of P starvation downregulated DEGs in wild-type and the upregulated DEGs in *d10* compared to wild-type. In total, 126 DEGs are SL repressed, independent of P starvation (Figure 3c). The dominant enriched terms for SL repressed genes, were 'sesquiterpenoid process', 'secondary shoot formation' and 'lactone biosynthetic- and metabolic process' including SL biosynthesis (Figure S4; Data S5). This suggests that these genes are overexpressed in *d10* as a result of a missing negative feedback regulation by SLs (Arite et al., 2007). In the overlapping region, there are 54 DEGs that are repressed by P starvation depending on the presence of SLs (Figure 3c). Among the 54 DEGs, there were many iron homeostasis-related genes. Intriguingly, *GIBBERELLIN 2-OXIDASE 2* (*GA2ox2*), catalyzing the degradation of active C_{19}-gibberellins (GAs) (Hedden, 2020), was upregulated in *d10* compared to wild-type (Data S5). Also, Wang, Duran, et al. (2021) found several *GA2ox* homologs being upregulated in a tomato *CCD8* RNAi mutant. It has been reported that GA regulates SL biosynthesis in rice via GA receptors, GIBBERELLIN INSENSITIVE DWARF1 (GID1) and GID2 (Ito et al., 2017). Furthermore, GA signaling repressor SLENDER RICE1 (SLR1) can interact with D14 in a SL-dependent manner (Nakamura et al., 2013). This suggests the existence of an interaction between the GA and SL signaling pathways (Marzec, 2017). Interestingly, rice overexpressing *GA2oxs*, including *GA2ox2*, displayed more tillering and a dwarf phenotype, just as SL-deficient mutants (Lo et al., 2008). The increased expression of *GA2ox2* we find here in *d10* suggests that SL represses *GA2ox2*, and hence GA catabolism, resulting in more active GA. However, there was no significant difference in the expression of GA biosynthetic genes in *d10* compared to wild-type under P starvation (Data S4). To further explore the interaction between SL and GA, we examined the expression pattern of GA pathway genes in GR24 treated roots (Figure S5, Data S6). GA biosynthetic gene *GA3ox2* ($\log_2$FC, 3.1) and GA catabolic gene *GA2ox2* ($\log_2$FC, 2.2) were significantly upregulated only in GR24 treated, P-sufficient *d10*, supporting the assumption that SL regulates tillering via fine-tuning of the GA pathway.

As already indicated above, 8 days of P starvation resulted in large changes in transcript levels. Among the top 10 strongest P starvation upregulated DEGs at day 8 were *ENT-KAURENE OXIDASE-LIKE* (7.8-fold), *PURPLE ACID PHOSPHATASE* (*PAP*) (5.1-fold), *PAP-LIKE* (6.7-fold), *SUCROSE-PHOSPHATASE LIKE* (3.2-fold) and *VACUOLAR PHOSPHATE EFFLUX TRANSPORTER* (*VPE*) (2.7-fold)

(Figure S6a). Unlike in tomato (Wang, Duran, et al., 2021), the induction of expression of these genes was quite similar in *d10*. *VPE* was also reported earlier to be involved in maintaining P homeostasis in rice (Oono et al., 2013; Secco et al., 2013). *PAP* genes have been shown to play a crucial role in plant adaptation to P starvation (Tian & Liao, 2015). All of the top 10 ranked P starvation-induced genes were strongly downregulated after 1 day of P resupply (Figure S6a).

The top 10 strongest downregulated DEGs upon P starvation were *FRUCTOSE-BISPHOSPHATE ALDOLASE*, *AMMONIUM TRANSPORTER -1;2* (*AMT1;2*), *ZINC FINGER, C2H2-TYPE DOMAIN*, *REGULATOR OF LEAF INCLINATION1* (*RLI1*) and several genes encoding uncharacterized proteins (Figure S6b). Consistent with this result, it was shown that the transcription factor SPX1 forms a complex with RLI1 to regulate rice leaf inclination in response to P availability. Under P deficient condition, *RLI* is repressed, which leads to reduced leaf angle (Ruan et al., 2018). Unlike in tomato (Wang, Duran, et al., 2021), the repression of these top P responsive genes in *d10* was similar to that in wild-type (Figure S6b).

To further pinpoint genes that respond specifically to SL, we analyzed the response to GR24. PCA showed that GR24 treatment affected transcript abundance under normal P (Figure S3). DEG analysis showed that GR24 treatment results in 291 upregulated and 172 downregulated genes (Figure 4a). These numbers decreased substantially under P starvation with only 156 upregulated and 78 downregulated genes as a result of GR24 treatment (Figure 4b, Data S7) and this is also reflected in the PCA (Figure S3). Interestingly, GR24 treatment in *d10* has a much stronger effect with 381 upregulated and 339 downregulated genes upon GR24 treatment under control P (Figure 4c), and 562 DEGs (226 up, 336 down with $\log_2FC \geq 1.2$, $P \leq 0.05$) under P deficiency (Figure 4d, Data S7) and this is also reflected in the larger shift in the *d10* expression profile upon GR24 treatment in Figure S3. This result is in line with previous reports on *Arabidopsis*, rice and tomato, showing that several P responsive genes compromised in SL mutants are restored with GR24 treatment (Gamir et al., 2020; Mayzlish-Gati et al., 2012; Sun et al., 2014). Because we used *rac*-GR24 (a mixture of $GR24^{5DS}$ and $GR24ent^{-5DS}$), which could potentially also trigger karrikin signaling via KARRIKIN INSENSITIVE2 (KAI2) (Scaffidi et al., 2014), we examined karrikin signaling genes. Interestingly, GR24 treatment did not affect the expression level of karrikin signaling genes in the roots (Figure S5; Data S8).

A group of genes induced by GR24 treatment shared the same GO terms with P starvation-induced genes, such as 'oxidation reduction', 'heme binding', 'oxidoreductase activity', 'tetrapyrrole binding' and 'catalytic activity'. On the other hand, genes involved in 'carboxylic'- and 'organic acid metabolic process', 'iron ion binding' and 'L-serine biosynthetic process' were enriched among the GR24 treatment upregulated genes but were not affected by P starvation (Data S9).

P starvation affects expression of carotenoid, ABA and strigolactone related genes

To further explore the effect of P starvation on the metabolism of SLs and related signaling molecules, such as ABA and zaxinone, we zoomed in on the carotenoid pathway. Carotenoids are formed from the condensation of the five-carbon isopentenyl diphosphate (IPP) and dimethylallyl diphosphate (DMAPP), which are derived from the plastid-localized MEP pathway (Moise et al., 2014). 1-DEOXY-D-XYLULOSE 5-PHOSPHATE SYNTHASE (DXS) and 1-DEOXY-D-XYLULOSE 5-PHOSPHATE REDUCTOISOMERASE (DXR) are considered to catalyze rate-limiting steps in the MEP pathway and to regulate carotenoid flux (Nisar et al., 2015; Sun et al., 2018). Indeed, *DXS3* was strongly induced upon P starvation at day 8, with transcript levels slightly higher in *d10* ($\log_2FC$, 4.2) than in wild-type ($\log_2FC$, 3.4) (Figure 5a). Intriguingly, *DXS3* expression was reduced in GR24 treated samples. This supression was particularly pronounced in GR24 treated, P-sufficient *d10*, suggesting that *DXS3* upregulation by P starvation is partially controlled by SL feedback (Figure 5b).

IPP and DMAPP form the precurors of geranylgeranyl diphosphate (GGPP) that is converted to phytoene by PHYTOENE SYNTHASE (PSY). Subsequently, phytoene is subjected to a complex set of desaturation and isomerization reactions catalyzed by PHYTOENE DESATURASE (PDS), ζ-CAROTENE ISOMERASE (Z-ISO), ζ-CAROTENE DESATURASE (ZDS) and CAROTENOID ISOMERASE (CRTISO), which lead to lycopene (Moise et al., 2014; Moreno et al., 2021). The cyclization of lycopene divides carotenoid biosynthesis into two pathways. One pathway involves LYCOPENE β- and ε-CYCLASES (LCYb and LCYe) and the CYP450 enzymes CYP97A and CYP97C, leading to α-carotene and lutein. The other pathway involves LCYb and is initiated by the formation of β-carotene, which serves as the precursor for the synthesis of ABA and SLs (Al-Babili & Bouwmeester, 2015; Jia et al., 2018). The expression of *PDS*, *ZDS1-like*, *CRTISO*, *LYCe* and *CYP97A4* was upregulated by P starvation, in both wild-type and *d10* (Figure 5a). Interestingly, transcript levels of *CRTISO*, *LYCe* and *CYP97A4* were strongly repressed upon 1 day of P resupply at day 8 (Figure 5a) but did not change in response to GR24 treatment (Figure 5b), suggesting that these genes are regulated by P, independent of SL (Figure 5a). We further observed a trend for *PSY1* and *CYP97A4* reduction in both wild-type and *d10* GR24 treated roots, although this was not significant (Figure 5b).

The key ABA biosynthesis gene *NCED2* was significantly downregulated upon P deficiency, whereas transcript levels of the ABA catabolic gene *ABA 8′-HYDROXYLASE 2*

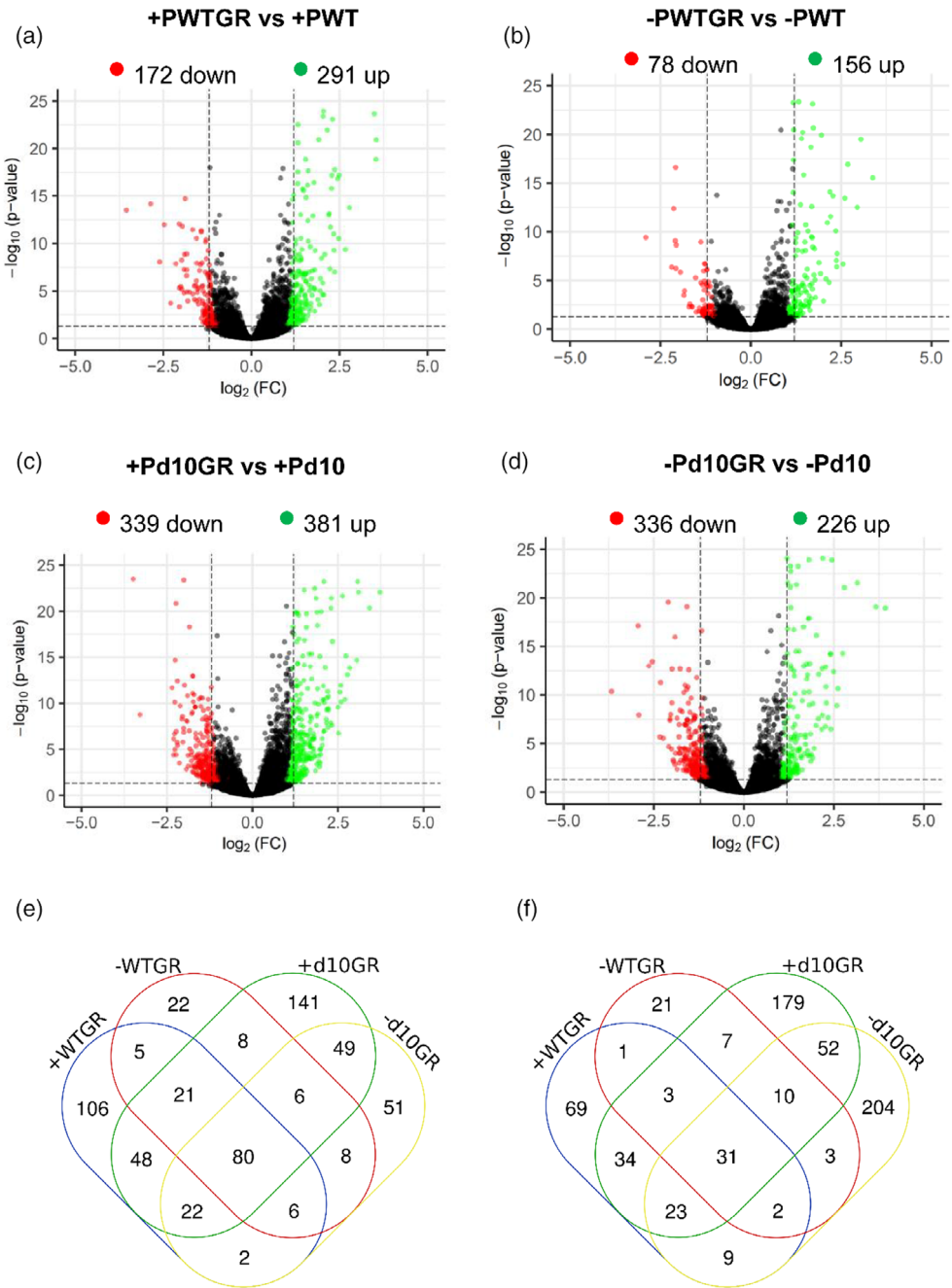

Figure 4. Number of significantly DEGs in wild-type and *d10* mutant in response to GR24 under both +P and –P at day 8.
(a, b) Volcano plots of 5 μM *rac*-GR24 treated wild-type roots compared to mock treated wild-type control under both +P (+PWTGR versus +PWT) and –P (–PWTGR versus –PWT) conditions, respectively. (c, d) Volcano plots of GR24 treated *d10* mutant roots compared to mock treated *d10* mutant control under both +P (+Pd10GR versus +Pd10) and –P (–Pd10GR versus –Pd10) conditions, respectively. Red dots indicate significant number of downregulated genes, green dots indicate significant number of upregulated genes and black dots indicate genes that did not pass the threshold filters. (e, f) Venn diagrams of (e) upregulated and (f) downregulated genes. +WTGR, –WTGR, +d10GR and –d10GR represent the DEGs of comparisons +PWTGR versus +PWT, –PWTGR versus –PWT, +Pd10GR versus +Pd10 and –Pd10GR versus –Pd10. $P < 0.05$; $\log_2 FC \geq 1.2$.

(*ABA8OH2*) showed the opposite pattern, being induced by P starvation (Figure 5a). Interestingly, the expression of several ABA biosynthetic genes, such as *BETA-CAROTENE HYDROXYLASE 2* (*BCH2*), *SIMILAR TO ALDEHYDE OXIDASE-2* (*AAO2-like*), *ALDEHYDE OXIDASE 3* (*AAO3*) and ABA receptor *PYRABACTIN RESISTANCE 1 LIKE/REGULATORY COMPONENTS OF ABA RECEPTOR 9* (*PYL/PCAR9*) tended to increase in both wild-type and *d10* GR24 treated roots. However, no difference was found in response to P starvation (Figure 5a,b). This suggests that

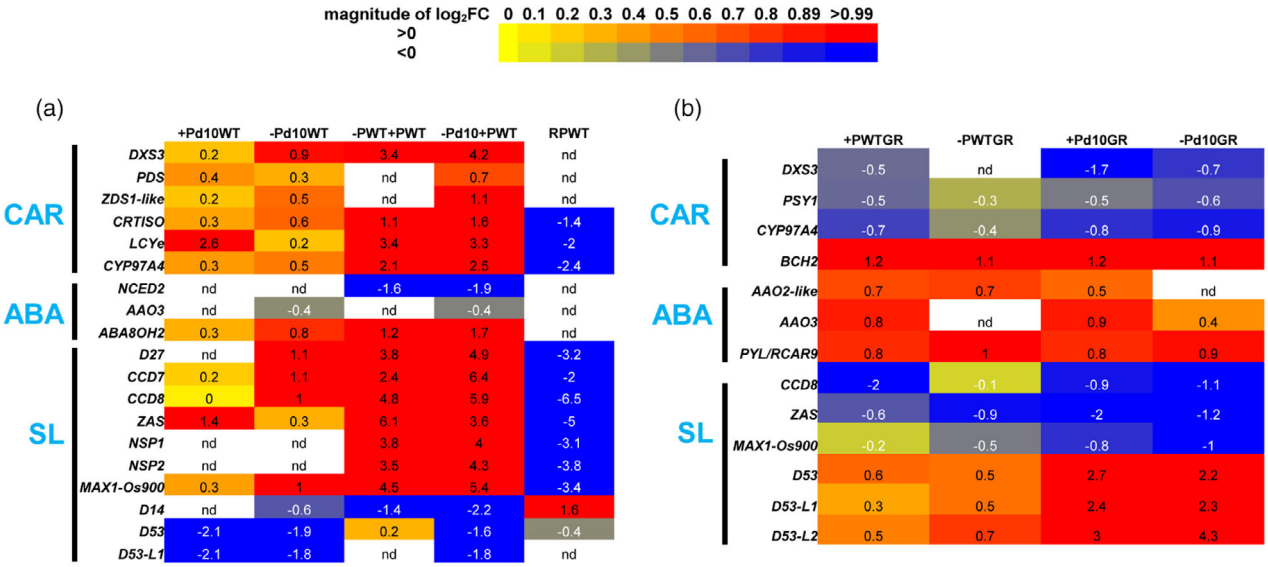

Figure 5. Heatmaps analysis of DEGs involved in carotenoid, ABA and SL pathways. (a) +Pd10WT, –Pd10WT, –PWT + PWT, –Pd10 + PWT and RPWT represent the DEGs of comparisons at day 8 + P*d10* versus +PWT, –P*d10* versus –PWT, –PWT versus +PWT, –P*d10* versus +PWT and RPWT versus –PWT, respectively. RP represents 1 day of +P resupply after 7 days of –P. (b) +PWTGR, –PWTGR, +Pd10GR and –Pd10GR represent the comparisons of +PWTGR24 versus +PWT, –PWTGR24 versus –PWT, +P*d10*GR versus +P*d10* and –P*d10*GR versus –P*d10*, respectively.

Carotenoid (CAR) pathway genes: *DXS3, 1-DEOXY-D-XYLULOSE 5-PHOSPHATE SYNTHASE3* (*Os07t0190000–01*); *PSY1, PHYTOENE SYNTHASE1* (*Os06t0729000–01*); *PDS, PHYTOENE DESATURASE* (*Os03t0184000–01*); *ZDS1-like, ζ-CAROTENE DESATURASE1-LIKE* (*Os07t0204900–01*); *CRTISO, CAROTENOID ISOMERASE* (*Os11t0572700–01*); *LCYe, ε-CYCLASES* (*Os01t0581300–01*); *CYP97A4, CAROTENOID β-RING HYDROXYLASE* (*Os02t0817900–01*); B*CH2, β-CAROTENE HYDROXYLASE2* (*Os04t0578400–01*).

ABA pathway genes: *NCED2, 9-cis-EPOXYCAROTENOID DIOXYGENASE2* (*Os12t0617400–01*); *AAO2-like, ALDEHYDE OXIDASE2-LIKE* (*Os07t0281700–01*); *AAO3, ALDEHYDE OXIDASE3* (*Os07t0282300–01*); *ABA8OH2, ABA 8′-HYDROXYLASE2* (*Os08t0472800–01*); *PYL/PCAR9, PYRABACTIN RESISTANCE 1 LIKE/REGULATORY COMPONENTS OF ABA RECEPTOR9* (*Os06t0562200–01*).

Strigolactone (SL) pathway genes: *D27, DWARF27* (*Os11t0587000–01*); *CCD7, CAROTENOID CLEAVAGE DIOXYGENASE7* (*Os04t0550600–01*); *CCD8, CAROTENOID CLEAVAGE DIOXYGENASE8* (*Os01t0746400–01*); *ZAS, ZAXINONE SYNTHASE* (*Os09t0321200–00*); *NSP1, NODULATION SIGNALING PATHWAY1* (*Os03t0408600–01*); *NSP2, NODULATION SIGNALING PATHWAY2* (*Os03t0263300–01*); *MAX1-Os900, MORE AXILLARY GROWTH1-CYP711A2* (*Os01t0700900–02*); *D14, DWARF14* (*Os03t0203200–01*); *D53, DWARF53* (*Os11t0104300–01*); *D53-L1, DWARF53-LIKE1* (*Os12t0104300–01*); *D53-L2, DWARF53-LIKE2* (*Os12t0104300–02*).

the ABA pathway is controlled by SL, independent of the presence of P.

SL biosynthetic genes *D27*, *CCD7*, *CCD8*, *MAX1-Os900*, SL biosynthesis regulators *NSP1*, *NSP2* and zaxinone biosynthetic gene *ZAS*, were highly induced by P starvation (Figure 5a). In particular, *CCD8*, *ZAS* and *MAX1-Os900* were suppressed in GR24 treated roots and this reduction was stronger in GR24 treated-*d10*. However, SL signaling repressors *D53*, *D53-L1* and *D53-L2* were strongly upregulated by GR24 application (Figure 5b). This clearly points towards the existence of a SL-regulated negative feedback mechanism. Taken together, we suggest that multiple genes involved in carotenoid, ABA and SL pathways work closely together in the regulation of P homeostasis.

Co-expression analysis revealed strigolactone biosynthesis candidate genes

SL biosynthesis in rice has only been partially resolved (Bouwmeester et al., 2021) and especially the origin and structure of the putative 'methoxy-5-deoxystrigol isomers' previously reported (Jamil et al., 2012) remain an enigma. Aiming to shed light on this, we performed co-expression analysis on the entire RNA-seq dataset using the known SL biosynthetic genes (*OsCCD7*, *OsCCD8* and *MAX1-Os900*) as baits. The 200 candidate genes were identified based on a co-expression network of all the genes in the dataset using the Pearson correlation coefficient (Figure 6a; Data S10). To further understand the biological role of these 200 candidates, GO analysis was performed, revealing that 'plastid and 'lipid metabolic process' were the most abundant terms (Figure 6b; Data S10). In the case of MF, 'phosphoric ester hydrolase activity' was the most enriched term followed by 'carotenoid dioxygenase activity'. Some major enrichment categories identified in BP, were 'isoprenoid biosynthetic process' including GA biosynthetic process, and phosphate ion transport (Figure 6b; Data S10). Hence, we conclude that transcriptional regulation of SLs by P availability plays an important role in coordinating the biosynthesis of isoprenoid-derived compounds.

Several CYP450s are involved in biosynthetic steps downstream of CL, which is the precursor of all canonical and non-canonical SLs (Bouwmeester et al., 2021). In rice, five CYP711 MAX1-homologs are known. MAX1-Os900

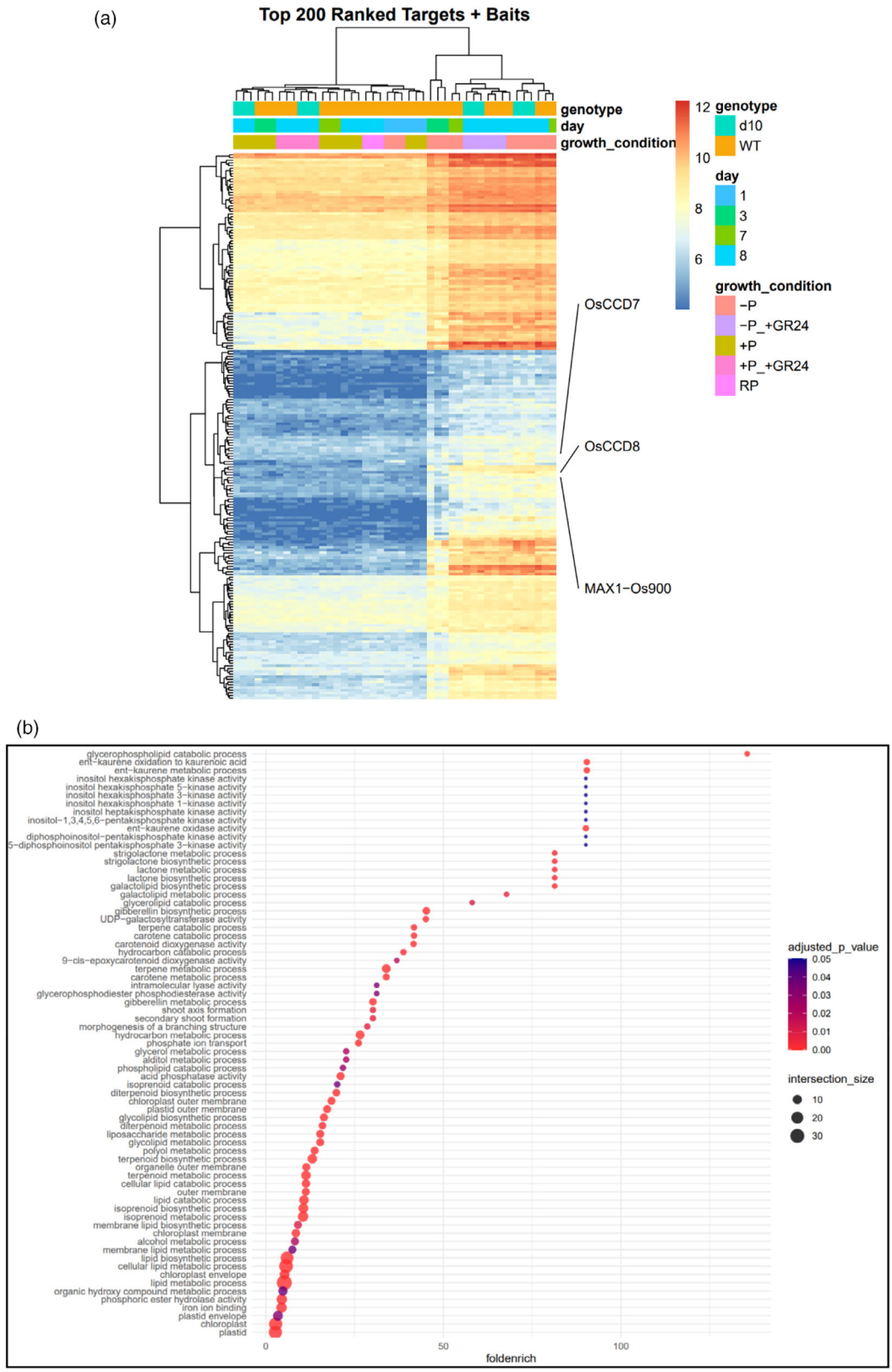

Figure 6. Gene co-expression network analysis of DEGs in wild-type and *d10* mutant in response to GR24 under both +P and −P using three SL bait genes. (a) Heatmap of top 200 ranked candidate with three SL baits genes. (b) GO enrichment analysis of top 200 ranked candidate with three SL baits genes. The size of the dots represents the number of enriched genes associated with GO term and the color of the dots represents adjusted *P*-values.

(CYP711A2) converts CL into 4-deoxyorobanchol (4DO), and MAX1-Os1400 (CYP711A3) catalyzes the subsequent hydroxylation of 4DO to form orobanchol (Zhang, Van Dijk, et al., 2014) (Figure 7c). Very recently, it was reported that *MAX1-Os900* knockout mutant lines lack the canonical SLs, 4DO and orobanchol, but do not display the high tillering shoot phenotype of mutants further upstream in the SL pathway such as *d27*, *d10* and *d17* (Figure 7c), suggesting that canonical SLs are not regulators of shoot branching in rice (Ito et al., 2022). In *Arabidopsis*, AtMAX1 catalyzes the formation of CLA from CL (Figure 7c) and CLA is then converted into MeCLA (Abe et al., 2014; Seto et al., 2014) by *Arabidopsis CLA METHYL TRANSFERASE* (*CLAMT*) (Mashiguchi et al., 2022). Among the co-expressed genes, we found three additional *CYP450s* genes and one putative *METHYL TRANSFERASE Os01g0700300* (Data S8). Interestingly, this *METHYL TRANSFERASE* was previously reported to be located close to *MAX1-Os900* (Cardoso et al., 2014). Based on a phylogenetic analysis, *METHYL TRANSFERASE Os01g0700300* shows high homology with *Os01g0701700*, and the two genes seem to have originated from a tandem duplication event (Wang, Li, et al., 2019). These two rice methyl transferases have been reported to be present in the same clade as *Arabidopsis CLAMT* (Mashiguchi et al., 2022), suggesting they may be involved in SL biosynthesis in rice, possibly in the production of the unidentified rice 'methoxy-5-deoxystrigol isomers' mentioned above. We therefore decided to focus on these *METHYL TRANSFERASES*.

Rice *METHYL TRANSFERASES* convert CLA into MeCLA

To characterize the two rice methyl transferase candidate genes, we transiently co-expressed them together with a CLA producing biosynthetic pathway in *N. benthamiana*.

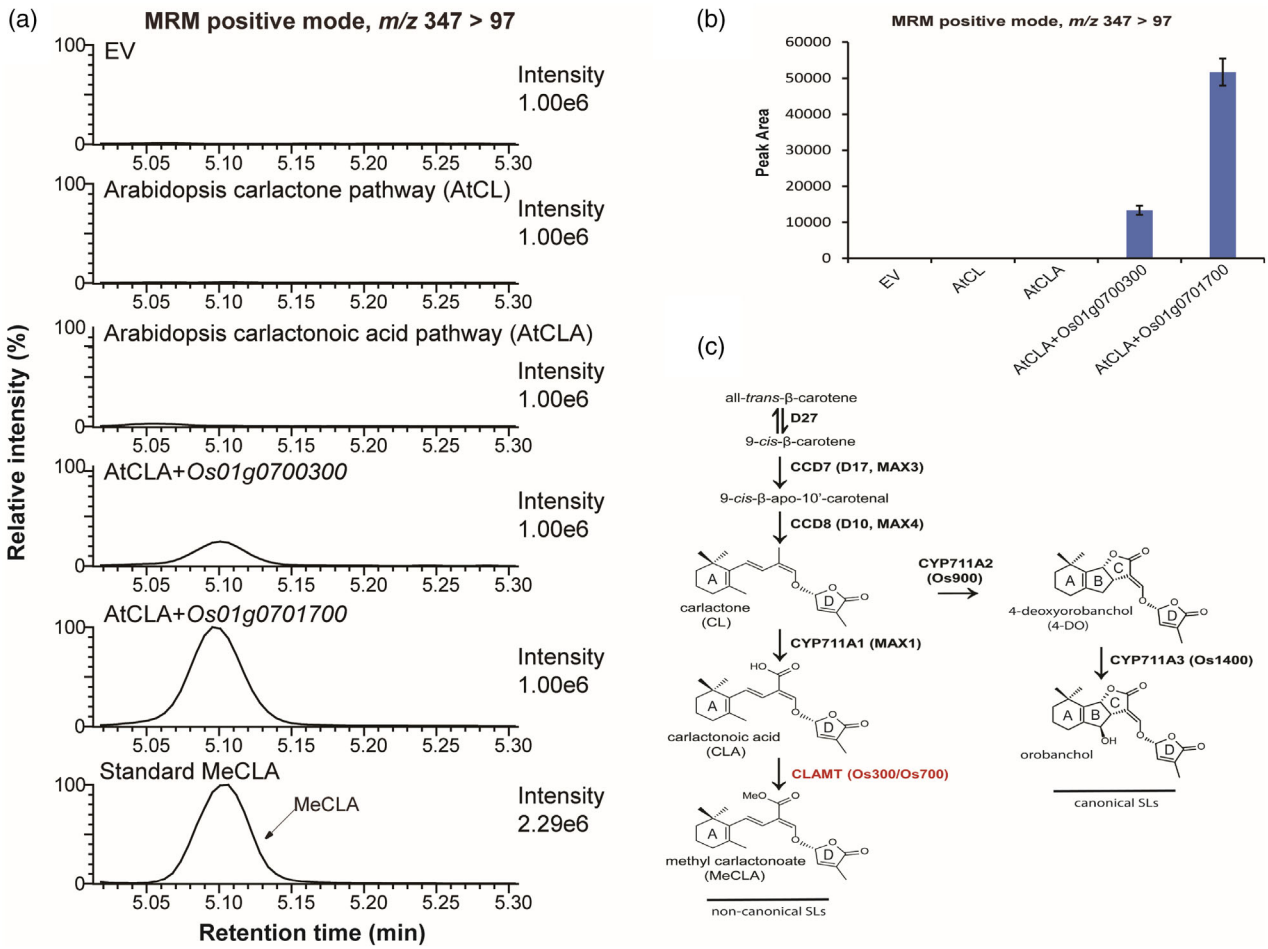

Figure 7. Production of methyl carlactonate (MeCLA) in transient expression assays using *Nicotiana benthamiana*.
(a) Representative MRM-LC/MS/MS chromatograms of MeCLA (transition $[M+H]^+$ *m/z* 347 > 97) in *N. benthamiana* leaf samples. (b) Quantification of MeCLA in *N. benthamiana* leaf samples. Data are shown as the mean ± SE (n = 5). EV, empty vector control; AtCL, *Arabidopsis* carlactone pathway genes (*AtD27*, *AtMAX3*, *AtMAX4*); AtCLA, *Arabidopsis* carlactonoic acid pathway (AtCL pathway + *AtMAX1*). (c) Biosynthetic pathway of canonical and non-canonical SLs in rice. The enzyme(s) identified in the present study is shown in red (bold). Abbreviations: D, Dwarf; CCD, CAROTENOID CLEAVAGE DIOXYGENASE; MAX, MORE AXILLARY GROWTH; CYP, cytochrome P450; CLAMT, CLA METHYL TRANSFERASE.

The Plant Journal published by Society for Experimental Biology and John Wiley & Sons Ltd.,
The Plant Journal, (2023), doi: 10.1111/tpj.16140

Because rice produces only a small amount of CLA from CL by *MAX1-Os900*/*Os1400* (Yoneyama et al., 2018), we co-expressed *AtMAX1* with the *Arabidopsis* CL pathway genes (*AtD27*, *AtMAX3* and *AtMAX4*) to generate CLA in *N. benthamiana* (Figure 7; Figure S7).

As anticipated, the transient expression of the *Arabidopsis* CL pathway genes resulted in the production of CL, which was consumed by *AtMAX1* to produce CLA (Figure S7). Furthermore, the agroinfiltration of either *Os01g0700300* or *Os01g0701700* together with the *Arabidopsis* CLA pathway led to the production of MeCLA (Figure 7). The quantity (according to the peak area) of MeCLA was almost three-fold higher when infiltrated with *Os01g0701700* than with *Os01g0700300*. Together, this indicates that both rice genes encode functional METHYL TRANSFERASES that catalyze the conversion of CLA into MeCLA, with *Os01g0701700* being more active than *Os01g0700300*. As discussed above, we also identified *CYP450s* genes in our co-expression data; perhaps these CYP450s use MeCLA as a substrate to produce downstream non-canonical SLs, such as the unidentified 'methoxy-5-deoxystrigol' isomers, but more work will be needed to confirm this.

CONCLUSIONS

Our work sheds light on the transcriptome reprogramming in response to P starvation in rice roots. We show that several genes involved in carotenoid, ABA and SL pathways are involved in the regulation of P homeostasis. Exploiting the generated dataset, we discovered a candidate SL biosynthetic gene using co-expression network analysis. Considering the importance of SLs in stress tolerance, this may ultimately benefit breeding to generate low P tolerant crops.

EXPERIMENTAL PROCEDURES

Plant materials

Wild-type Shiokari and the SL biosynthetic mutant *d10*, in the Shiokari background, were used in the present study. Rice seeds were surface sterilized with 70% ethanol for 30 sec and 2% sodium hypochlorite (v/v) for 30 min. The seeds were then rinsed five times in sterile double-distilled water and immersed in water in the dark for 2 days at 28°C to induce germination. Germinated seedlings were transferred to P sufficient (+P), modified half-strength Hoagland hydroponic solution (Wang, Haider, et al., 2019) and grown for 7 days in a climate room at 28°C day/22°C night (12 h light/dark photocycle) at 200 μM m^{-2} s^{-1} and 70% relative humidity. Subsequently, seedlings were transferred to +P or P deficient (–P) nutrient solution and harvested at 1, 3, 7 and 8 DAT (Figure S8). For P-replenishment treatment, after 7 days of P starvation, seedlings were re-supplied with P for 1 day. For the GR24 treatment, +P and –P seedlings after 7 days were treated with 5 μM *rac*-GR24 for 1 day. The nutrient solution was replaced every third day. Upon collection, roots samples were frozen in liquid nitrogen and then stored at −80°C until further analysis.

Total RNA isolation and library preparation

The total RNA from the roots tissues was extracted using TRIzol reagent (Invitrogen, Waltham, MA, USA) in accordance with the manufacturer's instructions. The integrity and quality of the total RNA were checked using DropSense™ (Trinean, Gentbrugge, Belgium). RNA was only used when $OD_{260/280}$ is higher than 1.8 and then $OD_{260/230}$ is higher than 2.0.

For RNA-seq library synthesis (three biological replicates per each condition and line combination, and two plants per replicate), a TruSeq® Stranded mRNA HT kit (RS-122-2103; Illumina Corp., San Diego, CA, USA) was used to prepare samples. An average of 96 libraries was multiplexed and loaded on each lane of the Illumina HiSeq flow cell. Sequencing was then performed on a HiSeq2500, with 125 bases paired-end run in accordance with the manufacturer's instructions (Illumina Corp.). An Agilent 2100 Bioanalyzer (Agilent, Santa Clara, CA, USA) was used for a library check. For library concentration, Pico green concentration measurement using a Tecan plate reader was performed (Tecan Group AG, Männedorf, Switzerland).

Mapping of RNA-seq reads and abundance estimation

BCL2FASTQ, version 2.17 (Illumina Corp.) was used for demultiplexing and fastq generation. Data were preprocessed using a SNAKEMAKE, version 5.2 (Köster & Rahmann, 2012) pipeline (Bliek et al., 2021). Reads were quality checked and trimmed using FASTP, version 0.19.5 (Chen et al., 2018). Then, they were mapped to Oryza sativa Japonica Group cultivar Nipponbare – IRGSP-1.0 from Rice Annotation Project Database (RAP-DB, http://rapdb.dna.affrc.go.jp) using STAR, version 2.7.6a (Dobin et al., 2013). Mapped reads were then assigned to transcript IDs using SUBREAD FEATURECOUNTS, version 1.6 (Liao et al., 2014). An overview of raw and -trimmed reads of all samples is provided in the mapping summary (Table S1).

Filtering, transformation and PCA

Further analyses were conducted in R, version 4.1 (R Core Team, 2021). Raw counts were filtered such that each transcript was required to be non-zero in all replicates in at least four experimental conditions. Counts were normalized for sequencing depth and transformed using DESEQ2 (Love et al., 2014). PCA was calculated in R and plotted using ggplot2, version 3.3.3 (https://ggplot2.tidyverse.org).

Differential expression (DE) analysis

DE analysis was performed using DESEQ2. Transcripts with greater than 1.2 absolute $\log_2$FC and adjusted $P < 0.05$ were considered differentially expressed, except for DEGs in the *d10* mutant compared to wild-type at 8 DAT for which $\log_2 FC \geq 1.0$ was used. Volcano plots were created using ENHANCEDVOLCANO, version 1.8 (https://github.com/kevinblighe/EnhancedVolcano).

Co-expression analysis

For co-expression analysis, Pearson correlation coefficients were calculated for all pairwise comparisons on the filtered transformed data. Three known SL biosynthetic genes *OsCCD7*, *OsCCD8* and *MAX1-Os900* were used to constrain this analysis. From these three genes, the others were ranked in order of highest positive correlation. The ranks for each gene were summed to create a joint rank. The top 200 were then considered as top candidates. These candidates were visualized using pheatmap, version 1.0.12 (https://rdrr.io/cran/pheatmap/).

GO enrichment analysis

GO enrichment analysis was performed using g:Profiler (http://biit.cs.ut.ee/gprofiler). The significance threshold (g:ScS) and level (0.05) were chosen as default. GO was performed on the output of the DE comparisons, as well as the two top candidate lists generated from the co-expression analysis. Furthermore, GO enrichment terms were visualized as dotplots in R.

Quantitative RT-PCR analysis

The first-strand cDNA was synthesized from 1 μg of total RNA using iScript™ cDNA synthesis Kit (Bio-Rad, Hercules, CA, USA) in accordance with the manufacturer's instructions. Primers specific to selected transcripts were designed using Integrated DNA Technologies (IDT) Inc. (Coralville, IA, USA) and qRT-PCR was performed using the SsoAdvanced™ Universal SYBR® Green Supermix (Bio-Rad) in accordance with the manufacturer's instructions, in a StepOnePlus™ Real-Time PCR System (Thermo Fisher Scientific). The rice *Ubiquitin* gene (*OsUBQ*) was used as an internal control to normalize target transcripts (Table S2). Quantitative relative expression values were calculated according to the $2^{-\Delta\Delta Ct}$ method and presented as the fold change (Livak & Schmittgen, 2001).

Transient expression in *Nicotiana benthamiana*

Arabidopsis genes (*AtD27*, *AtMAX3*, *AtMAX4* and *AtMAX1*) were cloned as previously described (Xu et al., 2021; Zhang, Van Dijk, et al., 2014). The full-length of two rice candidate genes (*Os01g0700300* and *Os01g0701700*) were amplified from cDNA of Nipponbare roots tissue using primers (Table S2). After sequence confirmation in the pJET1.2 vector (Fermentas, Waltham, MA, USA), cloning for agro-infiltration in *N. benthamiana* was conducted as previously reported into the binary vector pBINPLUS (van Engelen et al., 1995; Zhang, Van Dijk, et al., 2014), which was transformed into *Agrobacterium tumefaciens* strain AGL0. Transient expression was performed by agro-infiltration with combinations of *A. tumefaciens* batches containing the desired genes, using 1-month-old *N. benthamiana* plants (Zhang, Van Dijk, et al., 2014). Four biological replicates were used for each treatment. Five days after infiltration, infiltrated leaf samples were collected and stored at −80°C.

Strigolactone analysis

For CL, CLA and MeCLA analysis in *N. benthamiana* leaves, 200 mg of fine-ground leaf tissue was extracted with 1 mL of ethyl acetate. After vortexing and centrifuging, the supernatant was collected and the residue extracted once more. After drying the combined supernatants, 37.5 μL of ethyl acetate and 3 mL hexane were added to re-dissolve the residue. Strata® SI-1 Silica column (55 μm, 70 Å, 200 mg per 3 mL) (Phenomenex, Torrance, CA, USA) solid phase extraction was used for partial further purification of the strigolactones (Zhang, Van Dijk, et al., 2014). The resulting sample was dried using a SpeedVac (Thermo Fisher Scientific) and the residue dissolved in 200 μL of 25% acetonitrile, filtered over a nylon membrane filter (Thermo Fisher Scientific) and injected into the LC–MS/MS system. Targeted analysis of SLs was performed using MRM-LC–MS/MS (Floková et al., 2020). For quantification, representative MRM channels were chosen for CL, CLA and MeCLA (*m/z* 303 > 97, 331 > 113 and 347 > 97, respectively).

ACKNOWLEDGEMENTS

We thank Laurence Miesch for kindly providing MeCLA. This work was supported by NWO-grant on the role of strigolactones in the adaptation of rice to phosphate shortage (846.11.003; NSFC 11-08) to YZ, ERC Advanced Grant CHEMCOMRHIZO (670211) to HJB and Gravitation programme Harnessing the second genome of plants (MiCRop; Grant number 024.004.014, NWO/OCW) to HJB and IH, and baseline funding and Competitive Research Grant (CRG) to SA-B from King Abdullah University of Science and Technology (KAUST). We thank the Data Science Center at the University of Amsterdam.

AUTHOR CONTRIBUTIONS

HJB, SA-B and CR-S proposed the concept and designed the experiments. IH and ZY conducted experiments and prepared the RNA library for RNA-seq. FW, IH, ZY, RI, IA and TG analyzed RNA-seq data. IH performed qRT-PCR expression analysis. CL and IH conducted the *N. benthamiana* agroinfiltration assay and analyzed strigolactone content. IH, FW, CL and HJB wrote the manuscript. All authors read and approved the final version of the manuscript submitted for publication.

CONFLICT OF INTEREST

The authors declare no conflict of interest.

DATA AVAILABILITY STATEMENT

All data generated or analyzed during this study are included in the published article and the supplemental information.

SUPPORTING INFORMATION

Additional Supporting Information may be found in the online version of this article.

Data S1. List of DEGs in wild-type rice roots at different time points of P starvation (–P) and +P resupply.

Data S2. The log_2FC of DEGs showing in Heatmap in wild-type rice roots at different time points of P starvation and P resupply for top 10 *P Starvation Response* (*PSR*) genes and strigolactone biosynthetic and -signaling pathway genes.

Data S3. GO enrichment analysis of up and-down regulated DEGs at days 3, 7 and 8 upon P starvation compared to control P sufficient treatment in wild-type rice roots.

Data S4. List of DEGs in the *d10* mutant compared to wild-type under both +P and –P at day 8.

Data S5. GO enrichment analysis of wild-type and *d10* mutant roots under both +P and –P at day 8.

Data S6. List of DEGs involved in gibberellin pathway in wild-type and *d10* mutant roots in response to GR24 under both +P and –P at day 8.

Data S7. List of DEGs in wild-type and *d10* mutant roots in response to GR24 under both +P and –P at day 8.

Data S8. List of DEGs involved in karrikin signaling in wild-type and *d10* mutant roots in response to GR24 under both +P and –P at day 8.

Data S9. GO enrichment analysis of common DEGs in between wild-type and *d10* mutant roots in response to GR24 under both +P and –P at day 8.

Data S10. Go enrichment analysis of top 200 ranked candidate genes with three SL baits in wild-type and *d10* mutant roots in response to GR24 under both +P and –P.

Figure S1. Heatmaps showing the DEGs in wild-type rice roots at different time points of P starvation and +P resupply.

Figure S2. GO enrichment analysis of common DEGs after 7 days and 8 days of P starvation compared to control P sufficient treatment in wild-type rice roots.

Figure S3. PCA of rice roots transcript profiles using DEseq2 transformed counts in wild-type and *d10* mutant in response to GR24 under both +P and –P at day 8.

Figure S4. GO enrichment analysis of SL DEGs independent of P starvation at day 8.

Figure S5. Heatmaps analysis of DEGs involved in (a) gibberellin pathway and (b) karrikin signaling in response to GR24.

Figure S6. Heatmaps showing a strongest upregulated and downregulated DEGs in the roots of wild-type and *d10* mutant at day 8.

Figure S7. Production of carlactone (CL) and carlactonoic acid (CLA) in transient expression assays using *Nicotiana benthamiana*.

Figure S8. Schematic representation of the experimental design for RNA-seq.

Table S1. Mapping summary of RNA-seq experiment.

Table S2. Primer sequences used in the present study.

REFERENCES

Abe, S., Sado, A., Tanaka, K., Kisugi, T., Asami, K., Ota, S. *et al.* (2014) Carlactone is converted to carlactonoic acid by MAX1 in Arabidopsis and its methyl ester can directly interact with AtD14 in vitro. *Proceedings of the National Academy of Sciences of the United States of America*, **111**, 18084–18089.

Abel, S. (2017) Phosphate scouting by root tips. *Current Opinion in Plant Biology*, **39**, 168–177.

Abuauf, H., Haider, I., Jia, K.-P., Ablazov, A., Mi, J., Blilou, I. *et al.* (2018) The Arabidopsis DWARF27 gene encodes an all-trans-/9-cis-β-carotene isomerase and is induced by auxin, abscisic acid and phosphate deficiency. *Plant Science*, **277**, 33–42.

Al-Babili, S. & Bouwmeester, H.J. (2015) Strigolactones, a novel carotenoid-derived plant hormone. *Annual Review of Plant Biology*, **66**, 161–186.

Alder, A., Jamil, M., Marzorati, M., Bruno, M., Vermathen, M., Bigler, P. *et al.* (2012) The path from β-carotene to carlactone, a strigolactone-like plant hormone. *Science*, **335**, 1348–1351.

Aliche, E.B., Screpanti, C., De Mesmaeker, A., Munnik, T. & Bouwmeester, H.J. (2020) Science and application of strigolactones. *New Phytologist*, **227**, 1001–1011.

Arite, T., Iwata, H., Ohshima, K., Maekawa, M., Nakajima, M., Kojima, M. *et al.* (2007) DWARF10, an RMS1/MAX4/DAD1 ortholog, controls lateral bud outgrowth in rice. *The Plant Journal*, **51**, 1019–1029.

Bliek, T., Chouaref, J., van der Kloet, F. & Galland, M. (2021) *RNA-seq analysis pipeline (version 0.3.7)*. https://doi.org/10.5281/zenodo.4707140

Bouwmeester, H., Li, C., Thiombiano, B., Rahimi, M. & Dong, L. (2021) Adaptation of the parasitic plant lifecycle: germination is controlled by essential host signaling molecules. *Plant Physiology*, **185**, 1292–1308.

Brewer, P.B., Yoneyama, K., Filardo, F., Meyers, E., Scaffidi, A., Frickey, T. *et al.* (2016) LATERAL BRANCHING OXIDOREDUCTASE acts in the final stages of strigolactone biosynthesis in Arabidopsis. *Proceedings of the National Academy of Sciences of the United States of America*, **113**, 6301–6306.

Bruno, M. & Al-Babili, S. (2016) On the substrate specificity of the rice strigolactone biosynthesis enzyme DWARF27. *Planta*, **243**, 1429–1440.

Bruno, M., Hofmann, M., Vermathen, M., Alder, A., Beyer, P. & Al-Babili, S. (2014) On the substrate-and stereospecificity of the plant carotenoid cleavage dioxygenase 7. *FEBS Letters*, **588**, 1802–1807.

Bruno, M., Vermathen, M., Alder, A., Wüst, F., Schaub, P., van der Steen, R. *et al.* (2017) Insights into the formation of carlactone from in-depth analysis of the CCD 8-catalyzed reactions. *FEBS Letters*, **591**, 792–800.

Bürger, M. & Chory, J. (2020) The many models of strigolactone signaling. *Trends in Plant Science*, **25**, 395–405.

Cai, H., Xie, W. & Lian, X. (2013) Comparative analysis of differentially expressed genes in rice under nitrogen and phosphorus starvation stress conditions. *Plant Molecular Biology Reporter*, **31**, 160–173.

Cardoso, C., Zhang, Y., Jamil, M., Hepworth, J., Charnikhova, T., Dimkpa, S.O. *et al.* (2014) Natural variation of rice strigolactone biosynthesis is associated with the deletion of two MAX1 orthologs. *Proceedings of the National Academy of Sciences of the United States of America*, **111**, 2379–2384.

Chen, S., Zhou, Y., Chen, Y. & Gu, J. (2018) Fastp: an ultra-fast all-in-one FASTQ preprocessor. *Bioinformatics*, **34**, i884–i890.

Chien, P.-S., Chiang, C.-P., Leong, S.J. & Chiou, T.-J. (2018) Sensing and signaling of phosphate starvation: from local to long distance. *Plant and Cell Physiology*, **59**, 1714–1722.

Crombez, H., Motte, H. & Beeckman, T. (2019) Tackling plant phosphate starvation by the roots. *Developmental Cell*, **48**, 599–615.

Dell'Oste, V., Spyrakis, F. & Prandi, C. (2021) Strigolactones, from plants to human health: achievements and challenges. *Molecules*, **26**, 4579.

Dobin, A., Davis, C.A., Schlesinger, F., Drenkow, J., Zaleski, C., Jha, S. *et al.* (2013) STAR: ultrafast universal RNA-seq aligner. *Bioinformatics*, **29**, 15–21.

Floková, K., Shimels, M., Jimenez, B.A., Bardaro, N., Strnad, M., Novák, O. *et al.* (2020) An improved strategy to analyse strigolactones in complex sample matrices using UHPLC–MS/MS. *Plant Methods*, **16**, 1–17.

Gamir, J., Torres-Vera, R., Rial, C., Berrio, E., de Souza Campos, P.M., Varela, R.M. *et al.* (2020) Exogenous strigolactones impact metabolic profiles and phosphate starvation signalling in roots. *Plant, Cell & Environment*, **43**, 1655–1668.

Gho, Y.-S., An, G., Park, H.-M. & Jung, K.-H. (2018) A systemic view of phosphate starvation-responsive genes in rice roots to enhance phosphate use efficiency in rice. *Plant Biotechnology Reports*, **12**, 249–264.

Gu, M., Chen, A., Sun, S. & Xu, G. (2016) Complex regulation of plant phosphate transporters and the gap between molecular mechanisms and practical application: what is missing? *Molecular Plant*, **9**, 396–416.

Haider, I., Andreo-Jimenez, B., Bruno, M., Bimbo, A., Floková, K., Abuauf, H. *et al.* (2018) The interaction of strigolactones with abscisic acid during the drought response in rice. *Journal of Experimental Botany*, **69**, 2403–2414.

Ham, B.-K., Chen, J., Yan, Y. & Lucas, W.J. (2018) Insights into plant phosphate sensing and signaling. *Current Opinion in Biotechnology*, **49**, 1–9.

Hedden, P. (2020) The current status of research on gibberellin biosynthesis. *Plant and Cell Physiology*, **61**, 1832–1849.

Heuer, S., Gaxiola, R., Schilling, R., Herrera-Estrella, L., López-Arredondo, D., Wissuwa, M. *et al.* (2017) Improving phosphorus use efficiency: a complex trait with emerging opportunities. *The Plant Journal*, **90**, 868–885.

Hsieh, P.-H., Kan, C.-C., Wu, H.-Y., Yang, H.-C. & Hsieh, M.-H. (2018) Early molecular events associated with nitrogen deficiency in rice seedling roots. *Scientific Reports*, **8**, 1–23.

Ito, S., Bragu, y.J., Wang, J.Y., Yoda, A., Fiorilli, V., Takahashi, I. *et al.* (2022) Canonical strigolactones are not the major determinant of tillering but important rhizospheric signals in rice. *Science Advance*, **8**, eadd1278. Available from: https://doi.org/10.1126/sciadv.add1278

Ito, S., Yamagami, D., Umehara, M., Hanada, A., Yoshida, S. & Sasaki, Y. (2017) Regulation of strigolactone biosynthesis by gibberellin signaling. *Plant Physiology*, **174**, 1250–1259.

Jama-Rodzeńska, A., Białowiec, A., Koziel, J.A. & Sowiński, J. (2021) Waste to phosphorus: a transdisciplinary solution to P recovery from wastewater based on the TRIZ approach. *Journal of Environmental Management*, **287**, 112235.

Jamil, M., Charnikhova, T., Cardoso, C., Jamil, T., Ueno, K., Verstappen, F. *et al.* (2011) Quantification of the relationship between strigolactones and Striga hermonthica infection in rice under varying levels of nitrogen and phosphorus. *Weed Research*, **51**, 373–385.

Jamil, M., Charnikhova, T., Houshyani, B., van Ast, A. & Bouwmeester, H. (2012) Genetic variation in strigolactone production and tillering in rice and its effect on Striga hermonthica infection. *Planta*, **235**, 473–484.

Jeong, K., Baten, A., Waters, D.L., Pantoja, O., Julia, C.C., Wissuwa, M. *et al.* (2017) Phosphorus remobilization from rice flag leaves during grain filling: an RNA-seq study. *Plant Biotechnology Journal*, **15**, 15–26.

Jeong, K., Pantoja, O., Baten, A., Waters, D., Kretzschmar, T., Wissuwa, M. *et al.* (2018) Transcriptional response of rice flag leaves to restricted external phosphorus supply during grain filling in rice cv. IR6. *PloS one*, **13**, e0203654.

Jia, K.-P., Baz, L. & Al-Babili, S. (2018) From carotenoids to strigolactones. *Journal of Experimental Botany*, **69**, 2189–2204.

Jung, J.-Y., Ried, M.K., Hothorn, M. & Poirier, Y. (2018) Control of plant phosphate homeostasis by inositol pyrophosphates and the SPX domain. *Current Opinion in Biotechnology*, **49**, 156–162.

Kopriva, S. & Chu, C. (2018) Are we ready to improve phosphorus homeostasis in rice? *Journal of Experimental Botany*, **69**, 3515–3522.

Köster, J. & Rahmann, S. (2012) Snakemake—a scalable bioinformatics workflow engine. *Bioinformatics*, **28**, 2520–2522.

Lanfranco, L., Fiorilli, V., Venice, F. & Bonfante, P. (2018) Strigolactones cross the kingdoms: plants, fungi, and bacteria in the arbuscular mycorrhizal symbiosis. *Journal of Experimental Botany*, **69**, 2175–2188.

Liang, C., Wang, J., Zhao, J., Tian, J. & Liao, H. (2014) Control of phosphate homeostasis through gene regulation in crops. *Current Opinion in Plant Biology*, **21**, 59–66.

Liao, Y., Smyth, G.K. & Shi, W. (2014) featureCounts: an efficient general purpose program for assigning sequence reads to genomic features. *Bioinformatics*, **30**, 923–930.

Lin, H., Wang, R., Qian, Q., Yan, M., Meng, X., Fu, Z. *et al.* (2009) DWARF27, an iron-containing protein required for the biosynthesis of strigolactones, regulates rice tiller bud outgrowth. *The Plant Cell*, **21**, 1512–1525.

Liu, W., Kohlen, W., Lillo, A., Op den Camp, R., Ivanov, S., Hartog, M. *et al.* (2011) Strigolactone biosynthesis in Medicago truncatula and rice requires the symbiotic GRAS-type transcription factors NSP1 and NSP2. *The Plant Cell*, **23**, 3853–3865.

Livak, K.J. & Schmittgen, T.D. (2001) Analysis of relative gene expression data using real-time quantitative PCR and the 2− ΔΔCT method. *Methods*, **25**, 402–408.

Lo, S.F., Yang, S.Y., Chen, K.T., Hsing, Y.I., Zeevaart, J.A., Chen, L.J. *et al.* (2008) A novel class of gibberellin 2-oxidases control semidwarfism, tillering, and root development in rice. *The Plant Cell*, **20**, 2603–2618.

López-Arredondo, D.L., Leyva-González, M.A., González-Morales, S.I., López-Bucio, J. & Herrera-Estrella, L. (2014) Phosphate nutrition: improving low-phosphate tolerance in crops. *Annual Review of Plant Biology*, **65**, 95–123.

López-Ráez, J.A., Charnikhova, T., Gómez-Roldán, V., Matusova, R., Kohlen, W., De Vos, R. *et al.* (2008) Tomato strigolactones are derived from carotenoids and their biosynthesis is promoted by phosphate starvation. *New Phytologist*, **178**, 863–874.

López-Ráez, J.A., Shirasu, K. & Foo, E. (2017) Strigolactones in plant interactions with beneficial and detrimental organisms: the yin and Yang. *Trends in Plant Science*, **22**, 527–537.

Love, M.I., Huber, W. & Anders, S. (2014) Moderated estimation of fold change and dispersion for RNA-seq data with DESeq2. *Genome Biology*, **15**, 1–21.

Makhzoum, A., Yousefzadi, M., Malik, S., Gantet, P. & Tremouillaux-Guiller, J. (2017) Strigolactone biology: genes, functional genomics, epigenetics and applications. *Critical Reviews in Biotechnology*, **37**, 151–162.

Marzec, M. (2017) Strigolactones and gibberellins: a new couple in the phytohormone world? *Trends in Plant Science*, **22**, 813–815.

Mashiguchi, K., Seto, Y., Onozuka, Y., Suzuki, S., Takemoto, K., Wang, Y. *et al.* (2022) A carlactonoic acid methyltransferase that contributes to the inhibition of shoot branching in Arabidopsis. *Proceedings of the National Academy of Sciences of the United States of America*, **119**, e2111565119.

Matusova, R., Rani, K., Verstappen, F.W., Franssen, M.C., Beale, M.H. & Bouwmeester, H.J. (2005) The strigolactone germination stimulants of the plant-parasitic Striga and Orobanche spp. are derived from the carotenoid pathway. *Plant Physiology*, **139**, 920–934.

Mayzlish-Gati, E., De-Cuyper, C., Goormachtig, S., Beeckman, T., Vuylsteke, M., Brewer, P.B. *et al.* (2012) Strigolactones are involved in root response to low phosphate conditions in Arabidopsis. *Plant Physiology*, **160**, 1329–1341.

Medici, A., Szponarski, W., Dangeville, P., Safi, A., Dissanayake, I.M., Saenchai, C. *et al.* (2019) Identification of molecular integrators shows that nitrogen actively controls the phosphate starvation response in plants. *The Plant Cell*, **31**, 1171–1184.

Moise, A.R., Al-Babili, S. & Wurtzel, E.T. (2014) Mechanistic aspects of carotenoid biosynthesis. *Chemical Reviews*, **114**, 164–193.

Moreno, J.C., Mi, J., Alagoz, Y. & Al-Babili, S. (2021) Plant apocarotenoids: from retrograde signaling to interspecific communication. *The Plant Journal*, **105**, 351–375.

Mostofa, M.G., Li, W., Nguyen, K.H., Fujita, M. & Tran, L.S.P. (2018) Strigolactones in plant adaptation to abiotic stresses: An emerging avenue of plant research. *Plant, Eell & Environment*, **41**, 2227–2243.

Nakamura, H., Xue, Y.L., Miyakawa, T., Hou, F., Qin, H.M., Fukui, K. *et al.* (2013) Molecular mechanism of strigolactone perception by DWARF14. *Nature Communications*, **4**, 2613.

Nisar, N., Li, L., Lu, S., Khin, N.C. & Pogson, B.J. (2015) Carotenoid metabolism in plants. *Molecular Plant*, **8**, 68–82.

Oono, Y., Kawahara, Y., Kanamori, H., Mizuno, H., Yamagata, H., Yamamoto, M. *et al.* (2011) mRNA-Seq reveals a comprehensive transcriptome profile of rice under phosphate stress. *Rice*, **4**, 50–65.

Oono, Y., Kawahara, Y., Yazawa, T., Kanamori, H., Kuramata, M., Yamagata, H. *et al.* (2013) Diversity in the complexity of phosphate starvation transcriptomes among rice cultivars based on RNA-Seq profiles. *Plant Molecular Biology*, **83**, 523–537.

Pandey, A., Sharma, M. & Pandey, G.K. (2016) Corrigendum: emerging roles of Strigolactones in plant responses to stress and development. *Frontiers in Plant Science*, **7**, 860.

Puga, M.I., Rojas-Triana, M., de Lorenzo, L., Leyva, A., Rubio, V. & Paz-Ares, J. (2017) Novel signals in the regulation of pi starvation responses in plants: facts and promises. *Current Opinion in Plant Biology*, **39**, 40–49.

R Core Team. (2021) R: A language and environment for statistical computing. R Foundation for Statistical Computing, Vienna, Austria. https://www.R-project.org/

Rouached, H., Arpat, A.B. & Poirier, Y. (2010) Regulation of phosphate starvation responses in plants: signaling players and cross-talks. *Molecular Plant*, **3**, 288–299.

Ruan, W., Guo, M., Xu, L., Wang, X., Zhao, H., Wang, J. *et al.* (2018) An SPX-RLI1 module regulates leaf inclination in response to phosphate availability in rice. *The Plant Cell*, **30**, 853–870.

Scaffidi, A., Waters, M.T., Sun, Y.K., Skelton, B.W., Dixon, K.W., Ghisalberti, E.L. *et al.* (2014) Strigolactone hormones and their stereoisomers signal through two related receptor proteins to induce different physiological responses in Arabidopsis. *Plant Physiology*, **165**, 1221–1232.

Secco, D., Jabnoune, M., Walker, H., Shou, H., Wu, P., Poirier, Y. *et al.* (2013) Spatio-temporal transcript profiling of rice roots and shoots in response to phosphate starvation and recovery. *The Plant Cell*, **25**, 4285–4304.

Seto, Y., Sado, A., Asami, K., Hanada, A., Umehara, M., Akiyama, K. *et al.* (2014) Carlactone is an endogenous biosynthetic precursor for strigolactones. *Proceedings of the National Academy of Sciences of the United States of America*, **111**, 1640–1645.

Sun, H., Tao, J., Liu, S., Huang, S., Chen, S., Xie, X. *et al.* (2014) Strigolactones are involved in phosphate-and nitrate-deficiency-induced root development and auxin transport in rice. *Journal of Experimental Botany*, **65**, 6735–6746.

Sun, T., Yuan, H., Cao, H., Yazdani, M., Tadmor, Y. & Li, L. (2018) Carotenoid metabolism in plants: the role of plastids. *Molecular Plant*, **11**, 58–74.

Tian, J. & Liao, H. (2015) The role of intracellular and secreted purple acid phosphatases in plant phosphorus scavenging and recycling. *Annual Plant Reviews*, **48**, 265–287.

Umehara, M., Hanada, A., Magome, H., Takeda-Kamiya, N. & Yamaguchi, S. (2010) Contribution of strigolactones to the inhibition of tiller bud outgrowth under phosphate deficiency in rice. *Plant and Cell Physiology*, **51**, 1118–1126.

van Engelen, F.A., Molthoff, J.W., Conner, A.J., Nap, J.-P., Pereira, A. & Stiekema, W.J. (1995) pBINPLUS: an improved plant transformation vector based on pBIN19. *Transgenic Research*, **4**, 288–290.

Wang, B., Li, M., Yuan, Y. & Liu, S. (2019) Genome-wide comprehensive analysis of the SABATH gene family in Arabidopsis and rice. *Evolutionary Bioinformatics*, **15**, 1176934319860864.

Wang, J.Y., Haider, I., Jamil, M., Fiorilli, V., Saito, Y., Mi, J. *et al.* (2019) The apocarotenoid metabolite zaxinone regulates growth and strigolactone biosynthesis in rice. *Nature Communications*, **10**, 1–9.

Wang, Y., Duran, H.G.S., van Haarst, J.C., Schijlen, E.G., Ruyter-Spira, C., Medema, M.H. *et al.* (2021) The role of strigolactones in P deficiency induced transcriptional changes in tomato roots. *BMC Plant Biology*, **21**, 1–21.

Wang, Z., Kuo, H.-F. & Chiou, T.-J. (2021) Intracellular phosphate sensing and regulation of phosphate transport systems in plants. *Plant Physiology*, **187**, 2043–2055.

Waters, M.T., Gutjahr, C., Bennett, T. & Nelson, D.C. (2017) Strigolactone signaling and evolution. *Annual Review of Plant Biology*, **68**, 291–322.

Wild, R., Gerasimaite, R., Jung, J.-Y., Truffault, V., Pavlovic, I., Schmidt, A. *et al.* (2016) Control of eukaryotic phosphate homeostasis by inositol polyphosphate sensor domains. *Science*, **352**, 986–990.

Xu, X., Jibran, R., Wang, Y., Dong, L., Flokova, K., Esfandiari, A. *et al.* (2021) Strigolactones regulate sepal senescence in Arabidopsis. *Journal of Experimental Botany.*, **72**, 5462–5477.

Yang, X.J. & Finnegan, P.M. (2010) Regulation of phosphate starvation responses in higher plants. *Annals of Botany*, **105**, 513–526.

Yoneyama, K. & Brewer, P.B. (2021) Strigolactones, how are they synthesized to regulate plant growth and development? *Current Opinion in Plant Biology*, **63**, 102072.

Yoneyama, K., Mori, N., Sato, T., Yoda, A., Xie, X., Okamoto, M. *et al.* (2018) Conversion of carlactone to carlactonoic acid is a conserved function of MAX 1 homologs in strigolactone biosynthesis. *New Phytologist*, **218**, 1522–1533.

Zhang, Y., Van Dijk, A.D., Scaffidi, A., Flematti, G.R., Hofmann, M., Charnikhova, T. *et al.* (2014) Rice cytochrome P450 MAX1 homologs catalyze distinct steps in strigolactone biosynthesis. *Nature Chemical Biology*, **10**, 1028–1033.

Zhang, Z., Liao, H. & Lucas, W.J. (2014) Molecular mechanisms underlying phosphate sensing, signaling, and adaptation in plants. *Journal of Integrative Plant Biology*, **56**, 192–220.

Zhou, X., Liu, L., Li, Y., Li, K., Liu, X., Zhou, J. *et al.* (2020) Integrative metabolomic and transcriptomic analyses reveal metabolic changes and its molecular basis in rice mutants of the strigolactone pathway. *Metabolites*, **10**, 425.

Zhu, W., Yang, L., Yang, S., Gai, J. & Zhu, Y. (2016) Overexpression of rice phosphate transporter gene OsPT2 enhances nitrogen fixation and ammonium assimilation in transgenic soybean under phosphorus deficiency. *Journal of Plant Biology*, **59**, 172–181.